Large Low Shear Velocity ProvinceS
(LLSVPs)

Laura Cobden, Utrecht University

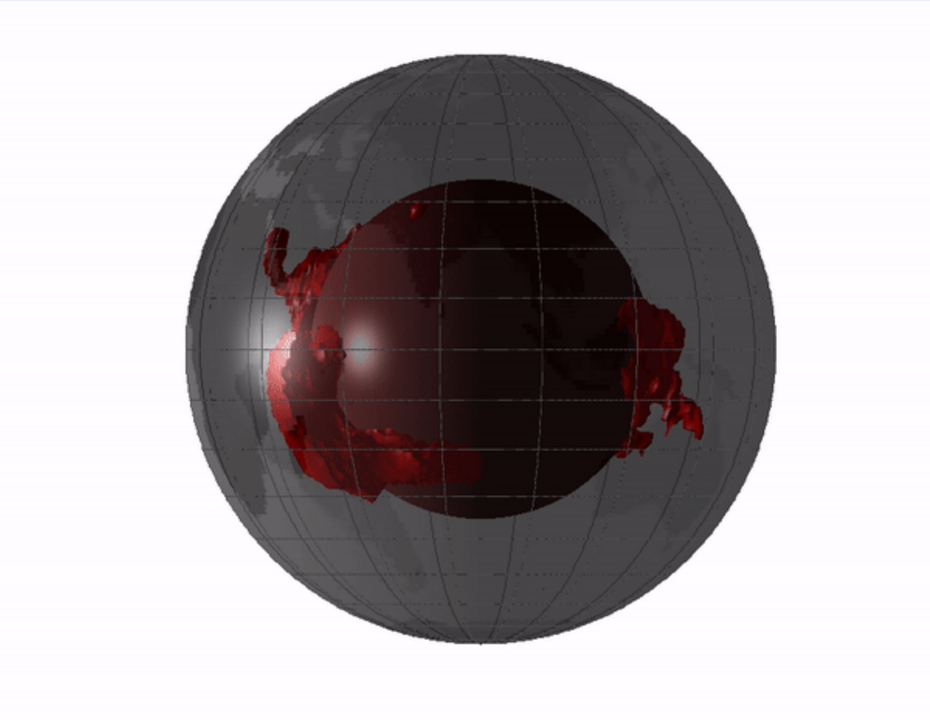

Animation from Cottaar & Lekic, 2016

HOT SPOTS

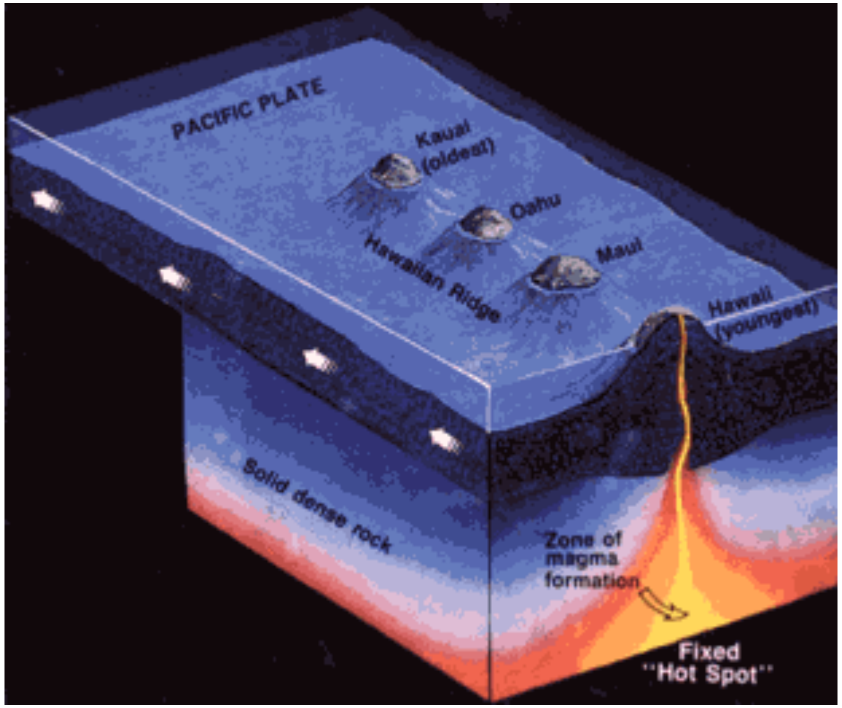

Figures borrowed from USGS

J. Tuzo Wilson, 1963

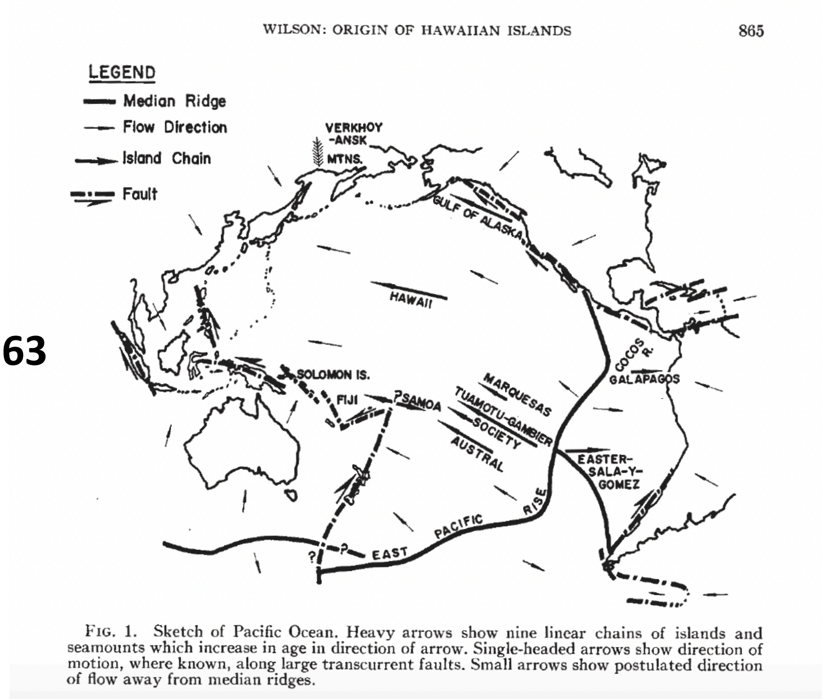

WILSON: ORIGIN OF HAWAIIAN ISLANDS 865

FIG. 1. Sketch of Pacific Ocean. Heavy arrows show nine linear chains of islands and seamounts which increase in age in direction of arrow. Single-headed arrows show direction of motion, where known, along large transcurrent faults. Small arrows show postulated direction of flow away from median ridges.

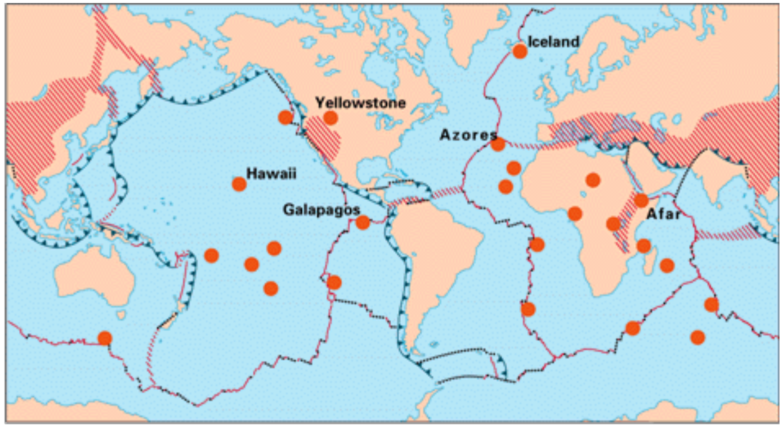

EXPLANATION

- **Divergent plate boundaries—Where new crust is generated as the plates pull away from each other.**
- **Convergent plate boundaries—Where crust is consumed in the Earth's interior as one plate dives under another.**
- **Transform plate boundaries—Where crust is neither produced nor destroyed as plates slide horizontally past each other.**
- ▨ **Plate boundary zones—Broad belts in which deformation is diffuse and boundaries are not well defined.**
- ● **Selected prominent hotspots**

MANTLE PLUMES

W. Jason Morgan, 1971

"It is assumed that hot spots are the surface expressions of deep mantle plumes roughly 150 km in diameter… extending to the deepest part of the mantle"

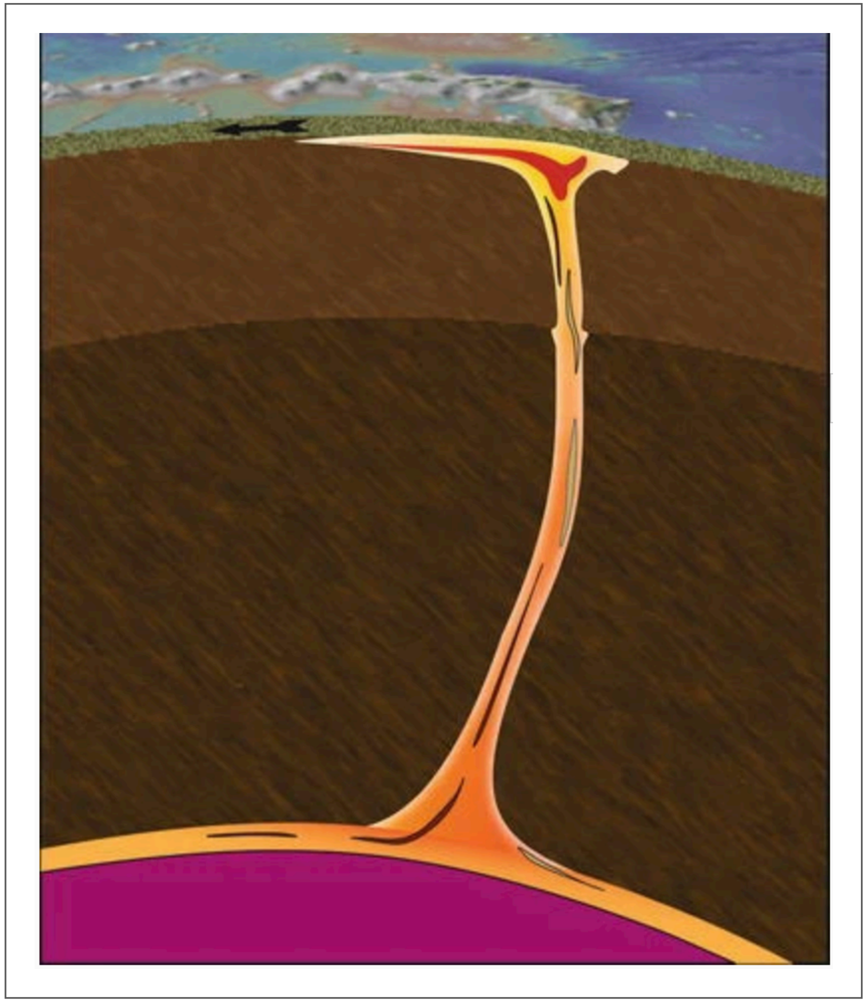

Image from White, 2016

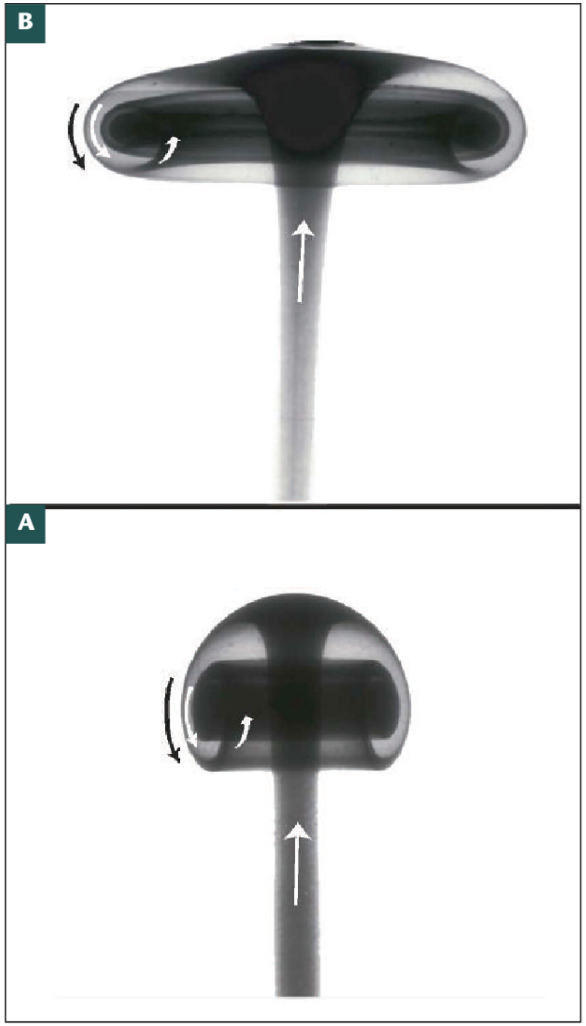

Photograph of a laboratory model of a starting thermal

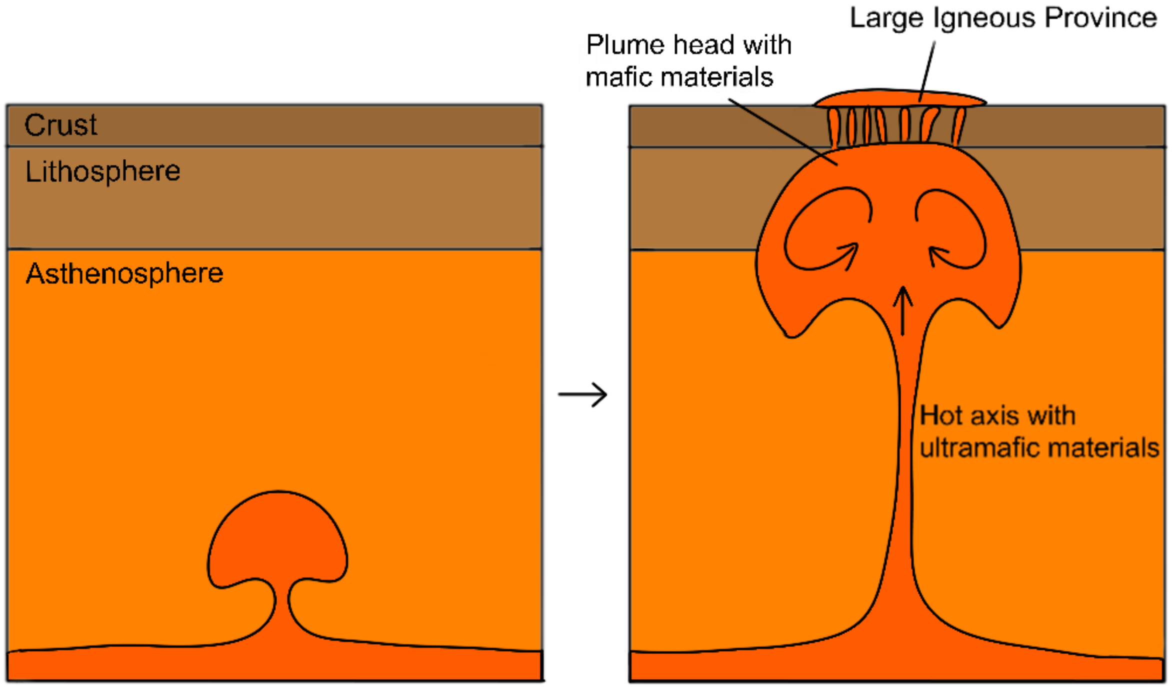


basalt
tuff
Bering Sea
St. Petersburg
Moscow
Volga R.
URAL MTS.
Ob R.
SIBERIAN TRAPS
Tungus R.
Ob R.
Umsk


Deccan Traps
India

Kilauea,
Hawaii

Eyjafjallajökull,
Iceland

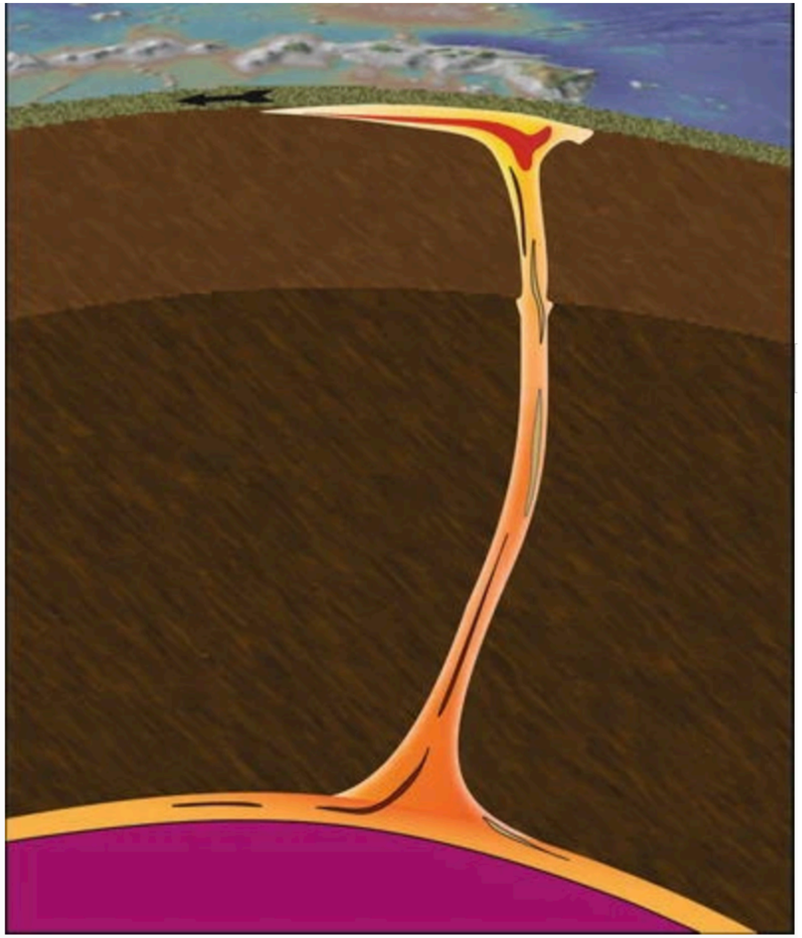

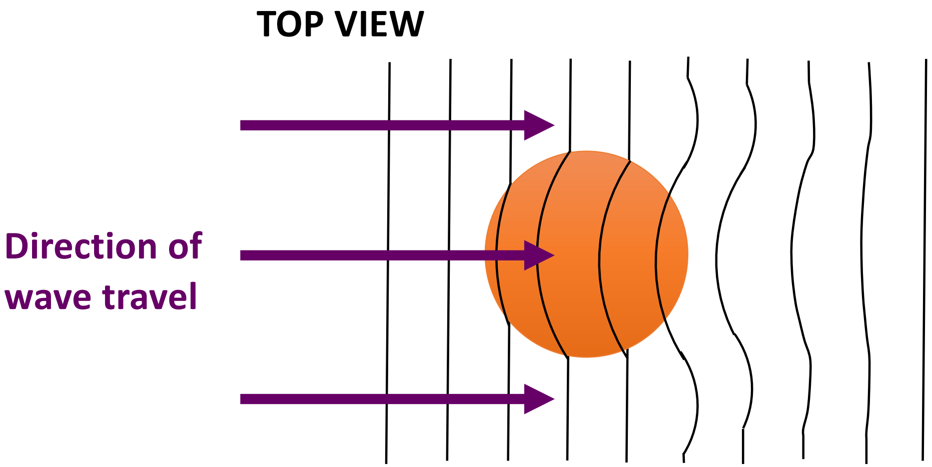

TOP VIEW

Direction of wave travel

Mantle plumes are notoriously difficult and controversial to image in seismology

This is often attributed to “wavefront healing”

Seismic tomography: Blue = fast, red = slow

First order assumption: blue = cold, red = hot

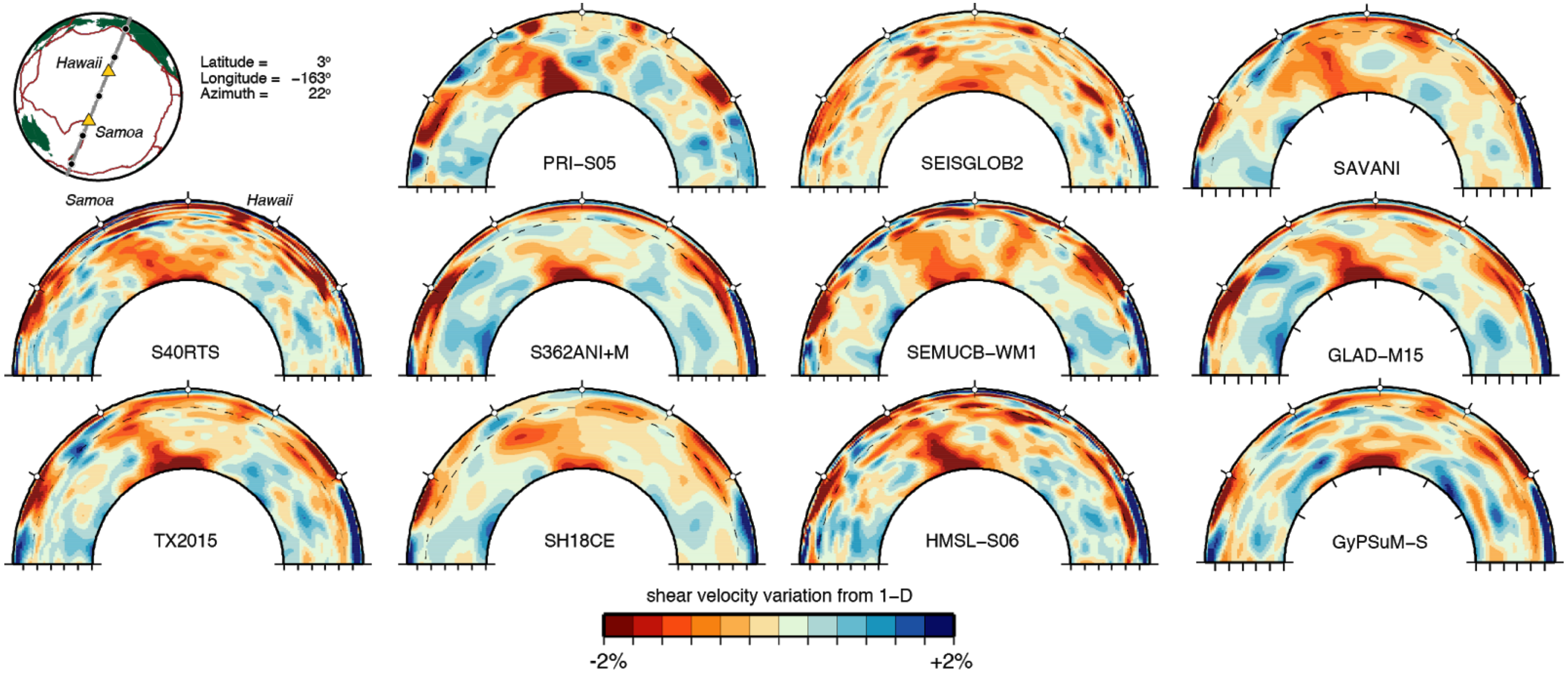

Compilation of different tomography models across the Pacific

Ritsema *et al*. 2021 (AGU monograph)

They all look quite different…..

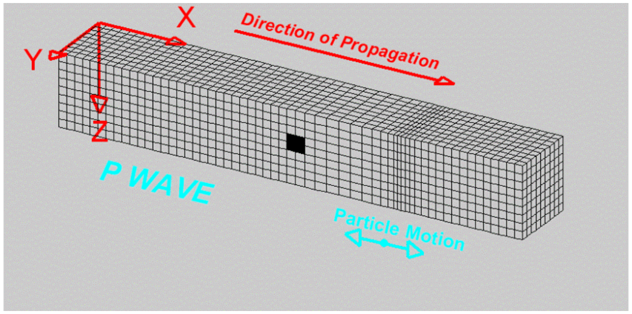

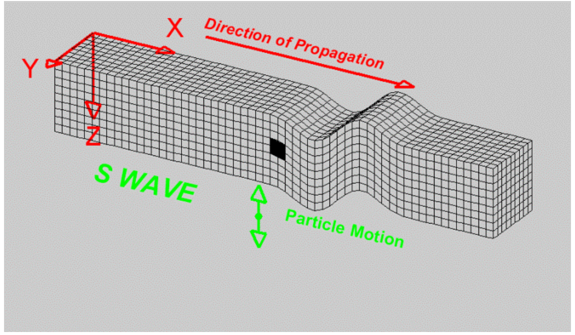

compressional wave speed
(P velocity, Vp)

2500 km depth

shear wave speed
(S velocity, Vs)

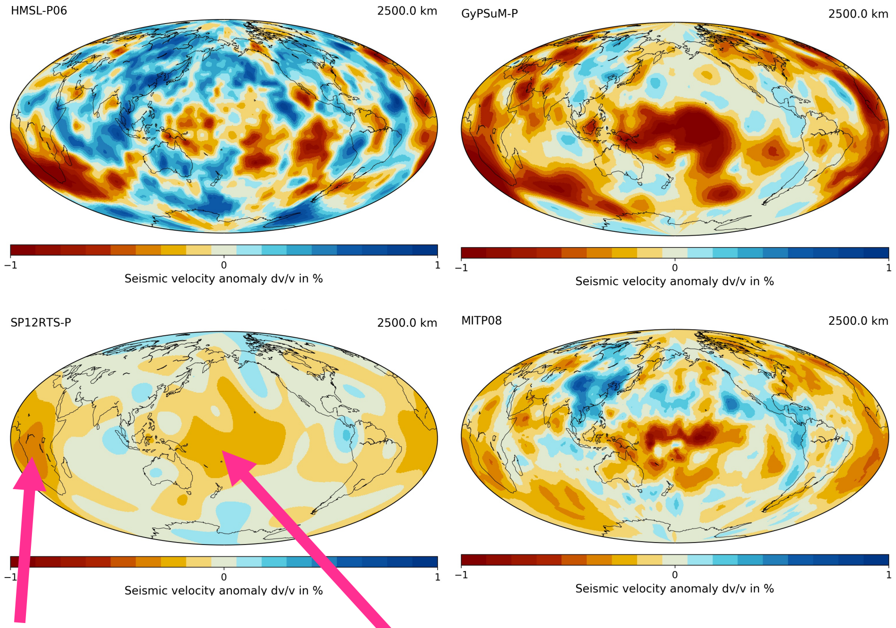

AFRICA

PACIFIC

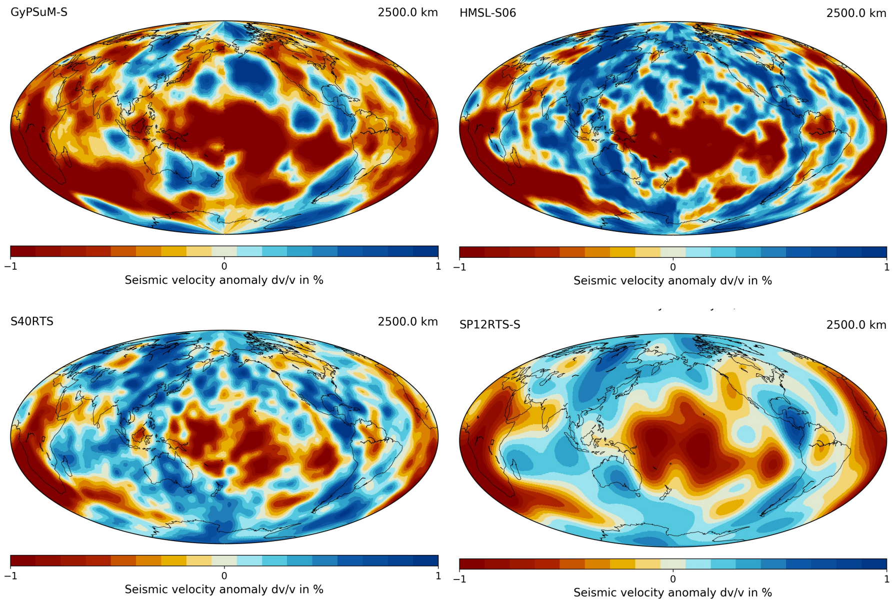

Seismic tomography models DO agree at large length scales

P-wave speed at 2300 km depth

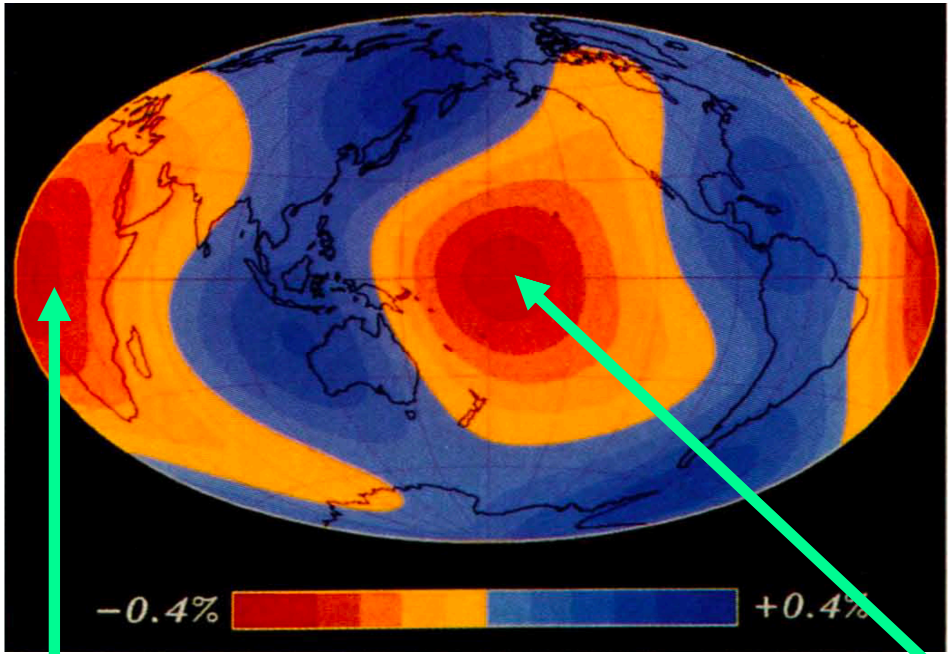

AFRICA

PACIFIC

Dziewonski & Woodhouse, 1987

Red = slow

Observed geoid

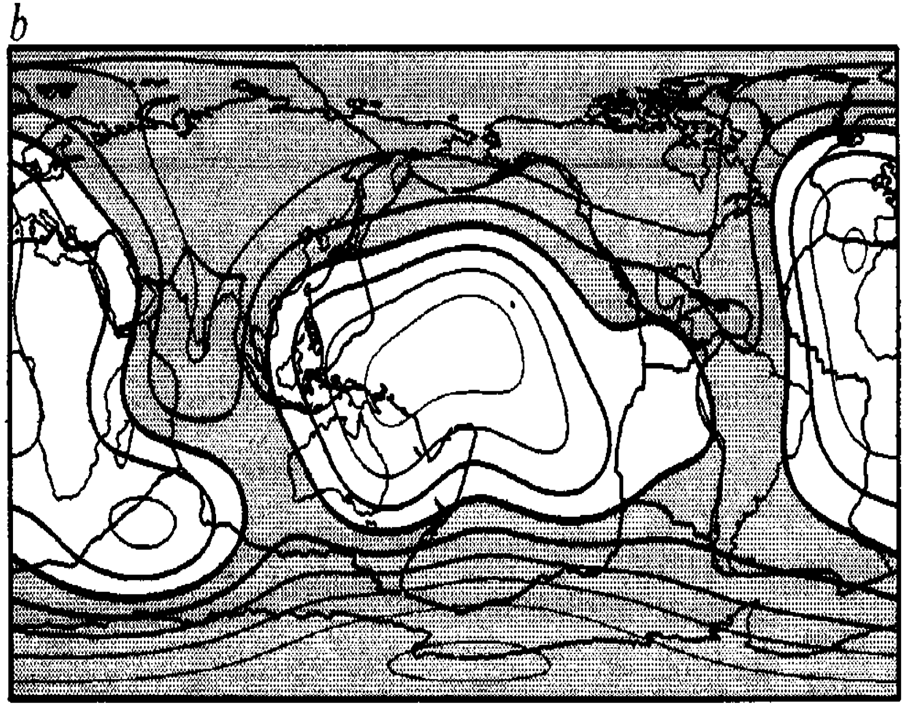

Hager et al., 1985

Geoid highs are white

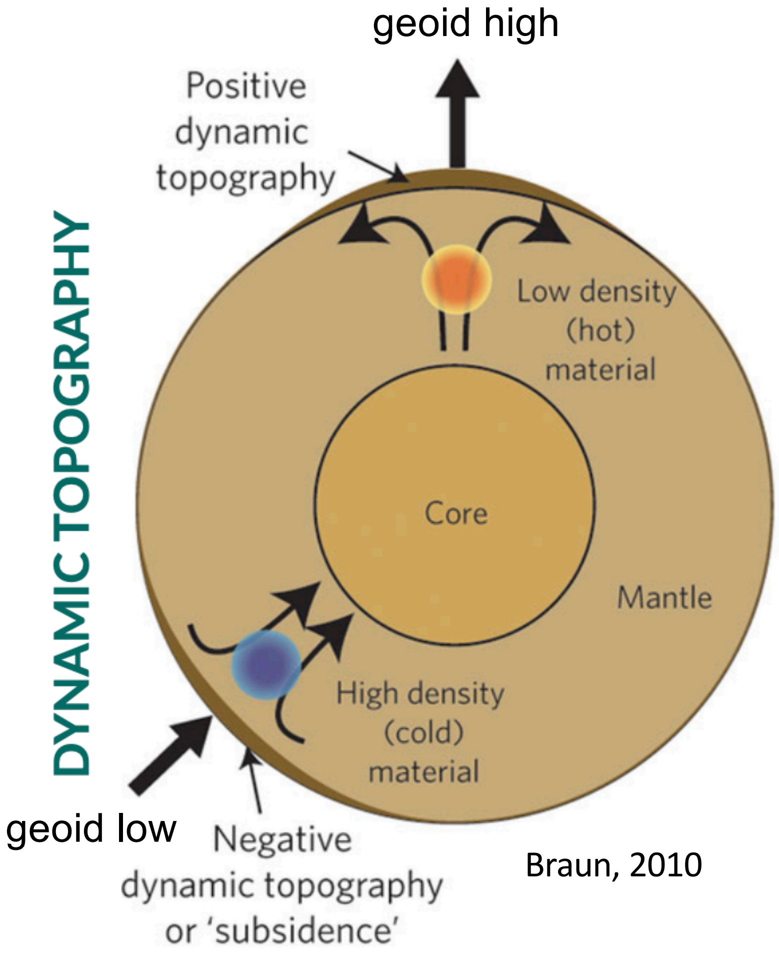

Braun, 2010

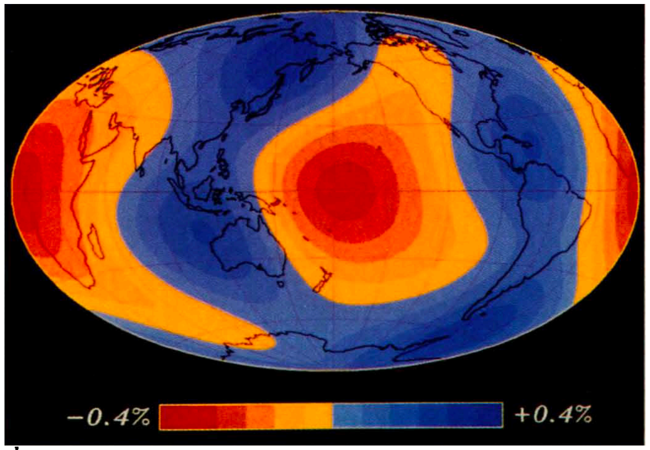

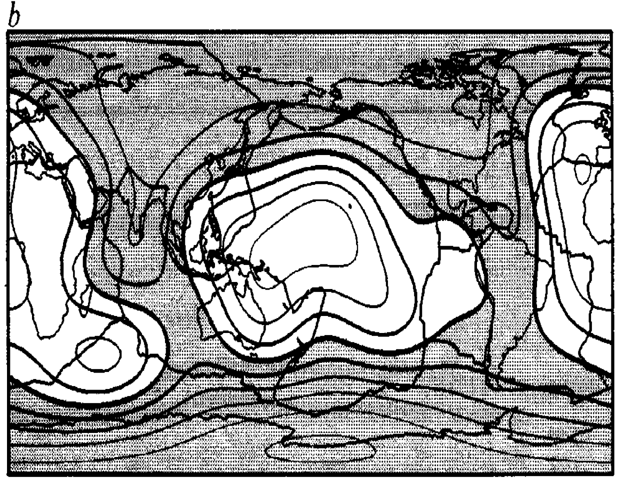

red = slow

Assume

= hot

= less dense

= buoyant

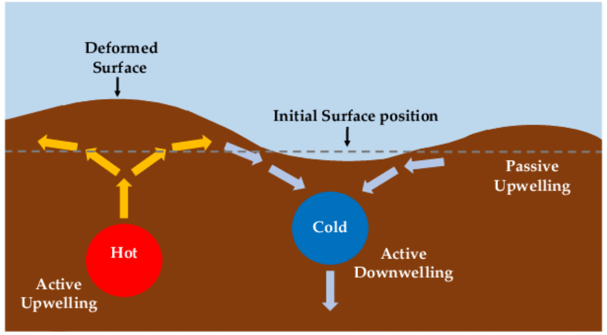

P-wave speed at 2300 km depth

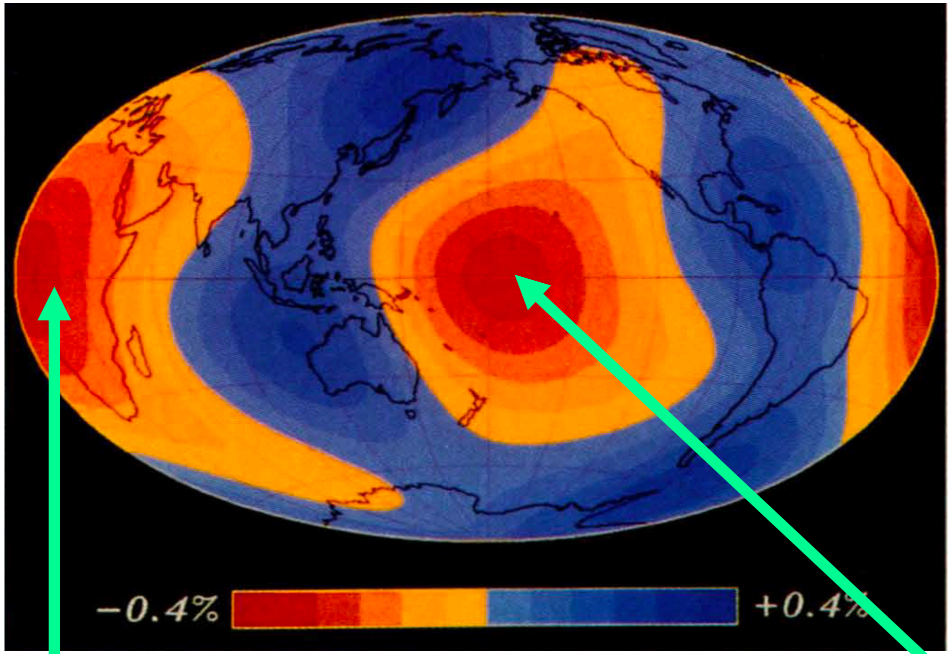

Dziewonski & Woodhouse, 1987

Observed geoid

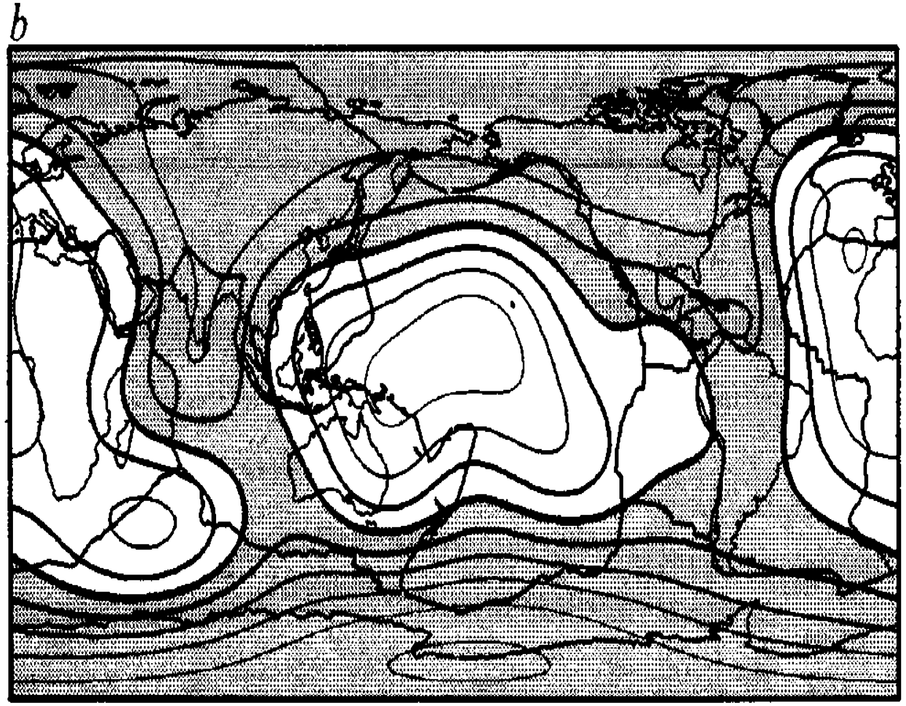

Hager et al., 1985

AFRICA

'superplume'

PACIFIC

'superplume'

D.R. Davies et al. / Earth and Planetary Science Letters 411 (2015) 121–130

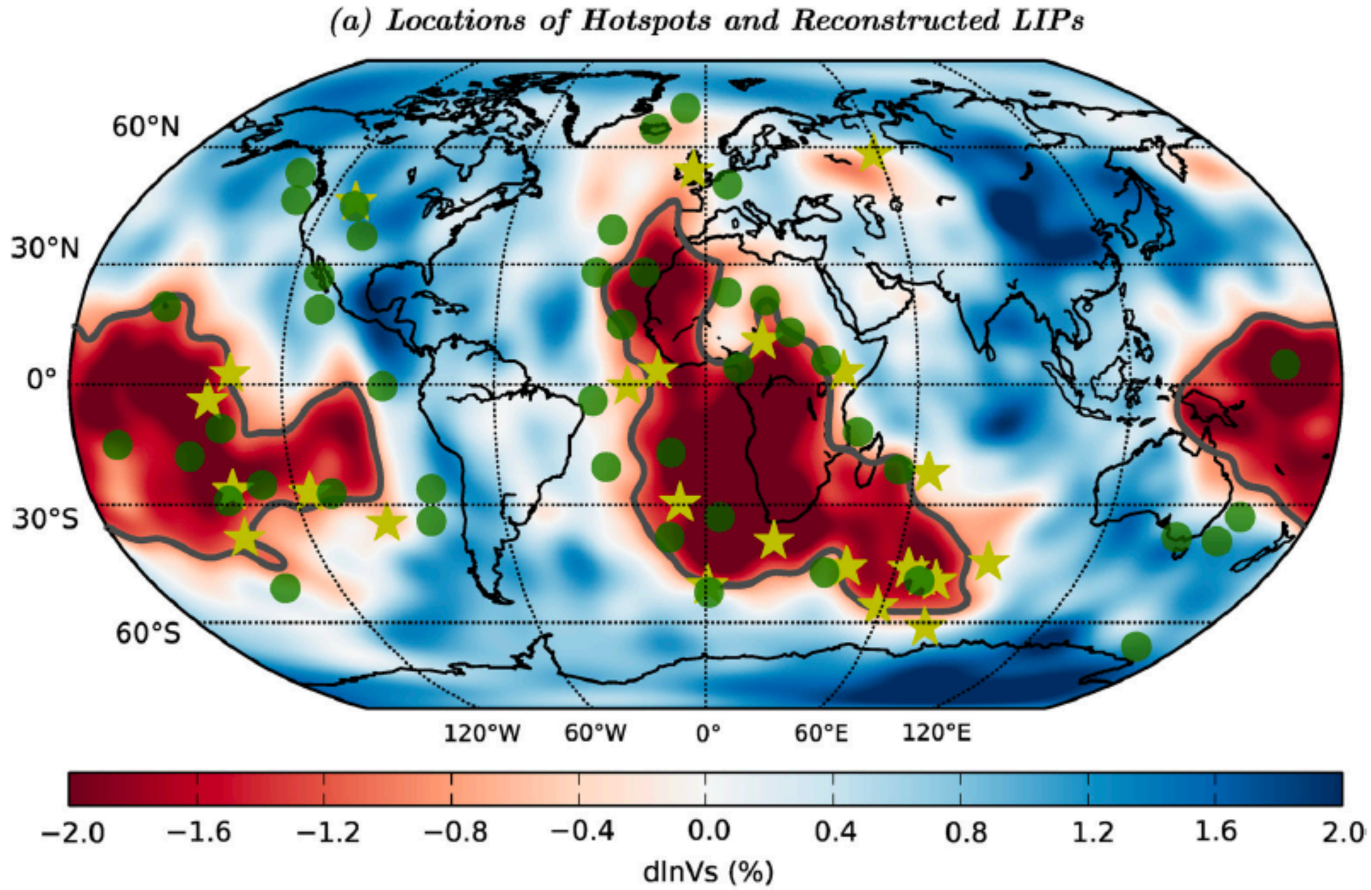

High concentration of hotspots (green circles) and reconstructed eruption sites of large igneous provinces (yellow stars) above the superplumes suggests a causal relation

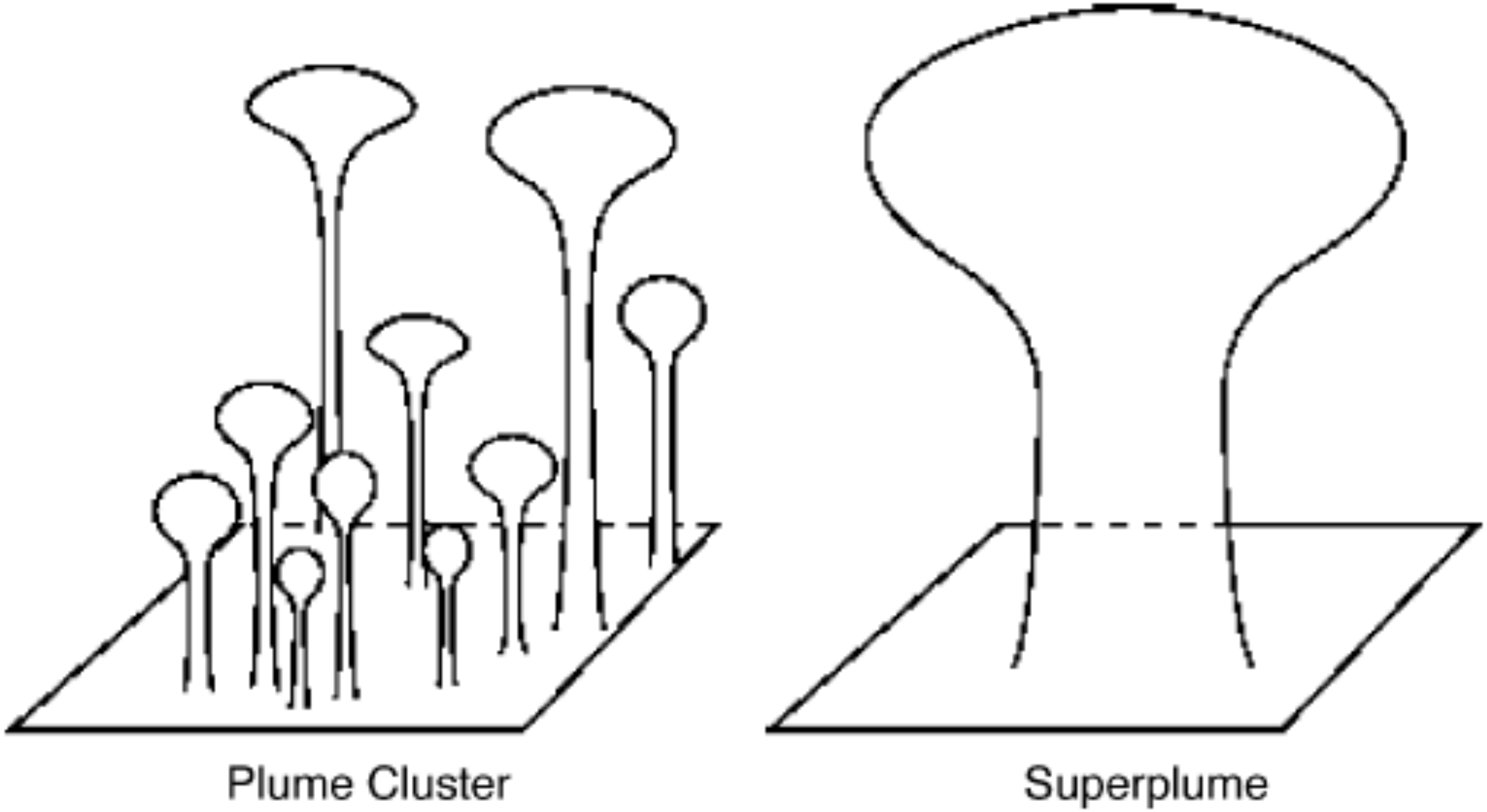

Fig. 6. Sketch of a plume cluster and a superplume.

Numerical modelling of thermochemical plumes

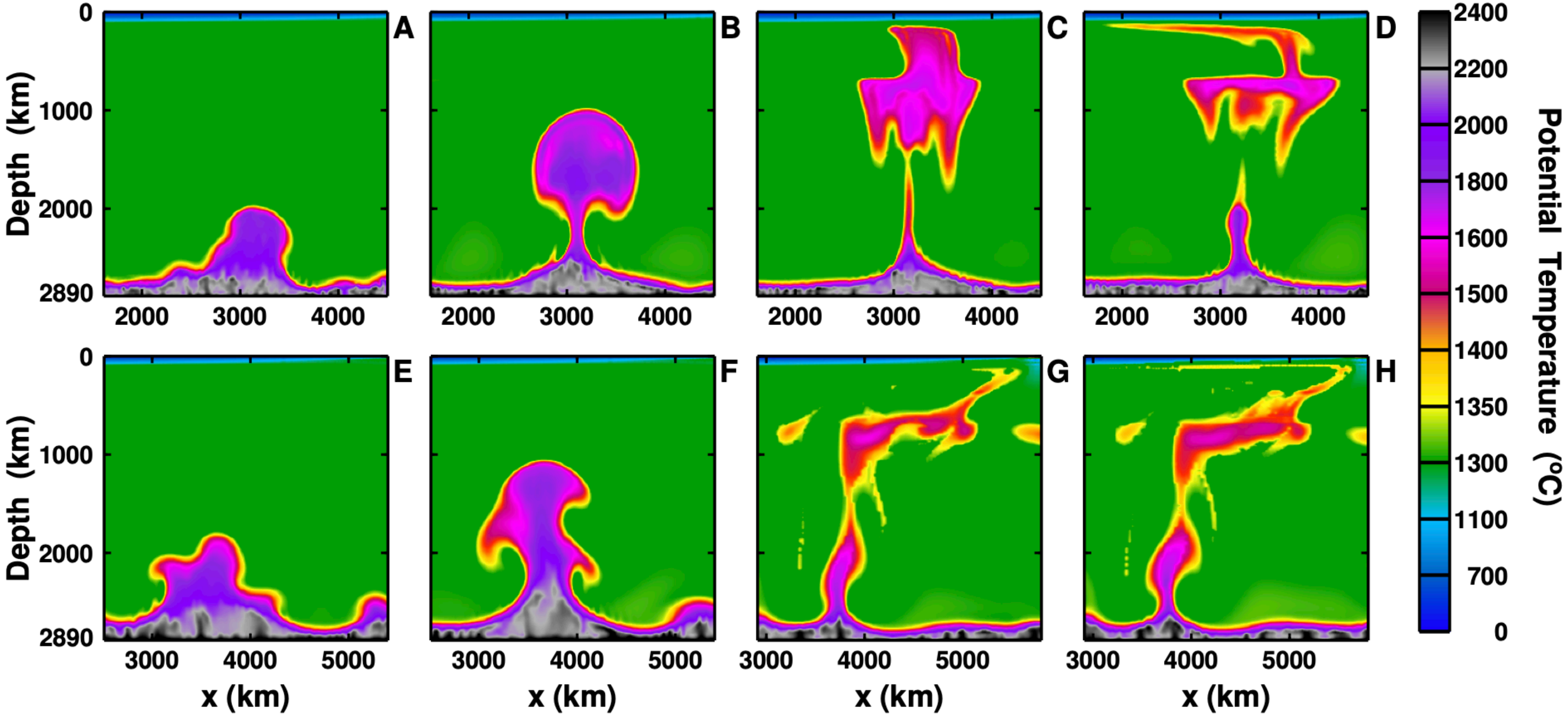

Laboratory modelling of thermochemical convection

Davaille, Nature 1999

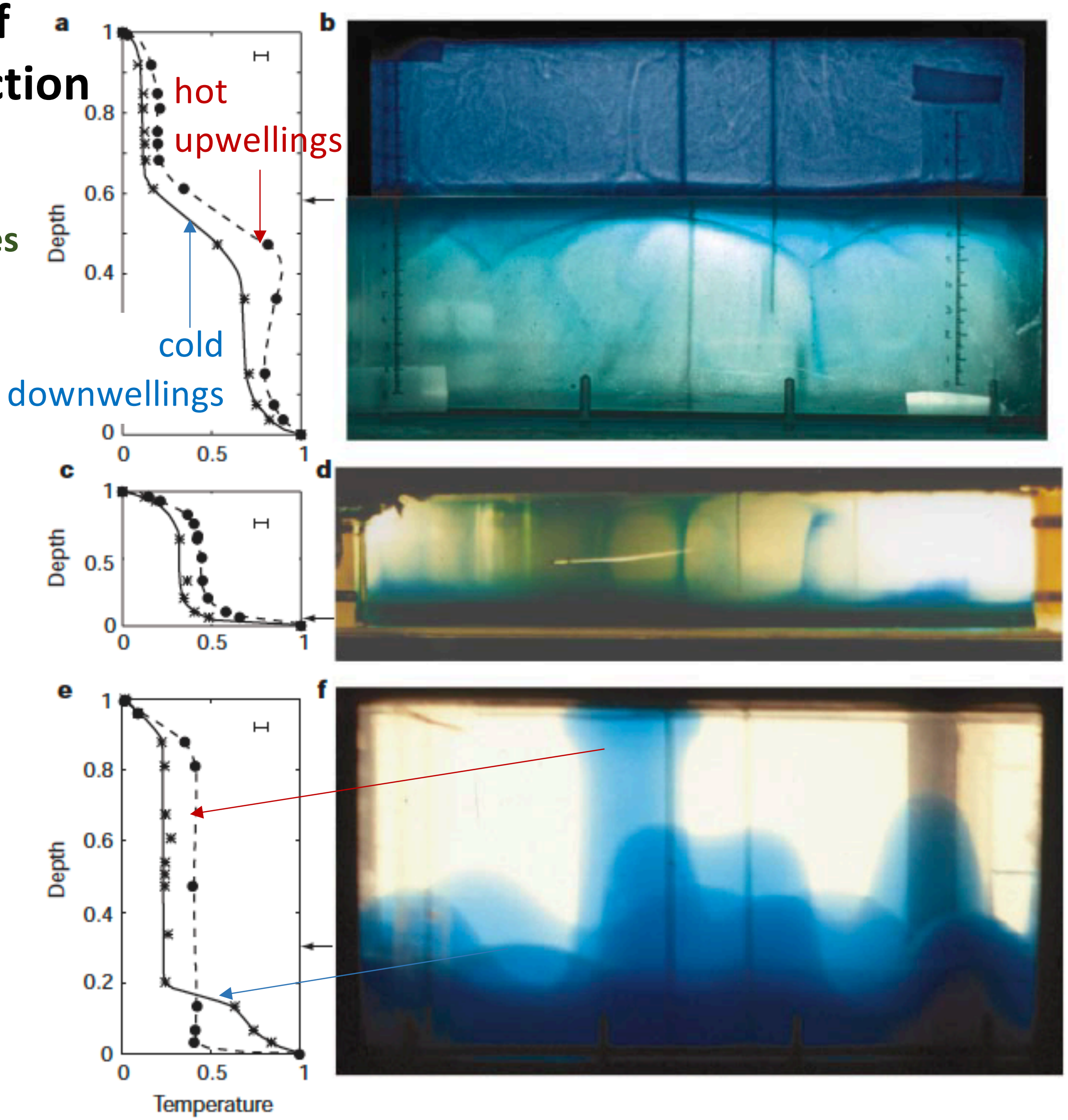

Two-layer convection with thin, tubular plumes rising from the interface

Strong viscosity stratification, thick bottom layer

Thin, tubular plumes (a la Morgan, 1971)

Strong stratification, thin bottom layer

Oscillating domes

Weak stratification

Ishii & Tromp, 1999

Seismic structure at 2800 km depth

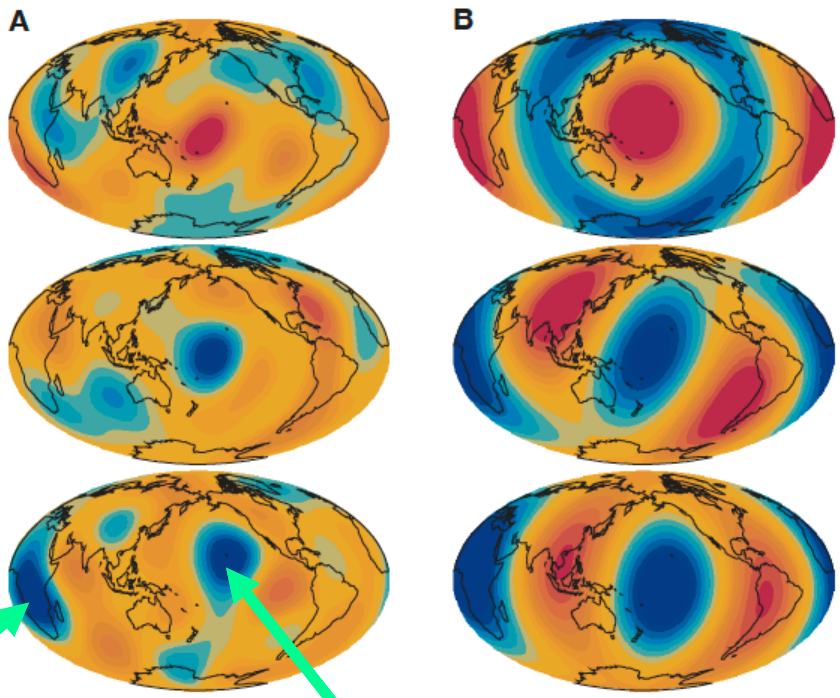

spherical harmonic degrees 2,4,6

degree 2 only

bulk modulus

shear modulus

$$V_P = \sqrt{\frac{K + \frac{4}{3} G}{\rho}}$$

P-wave velocity

$$V_S = \sqrt{\frac{G}{\rho}}$$

shear velocity

density

$$V_B = \sqrt{\frac{K}{\rho}}$$

Bulk sound velocity

$$V_B{}^2 = V_P{}^2 - \frac{4}{3} V_S{}^2$$

Can be retrieved by combining V_p and V_s

Ishii & Tromp, 1999

Seismic structure at 2800 km depth

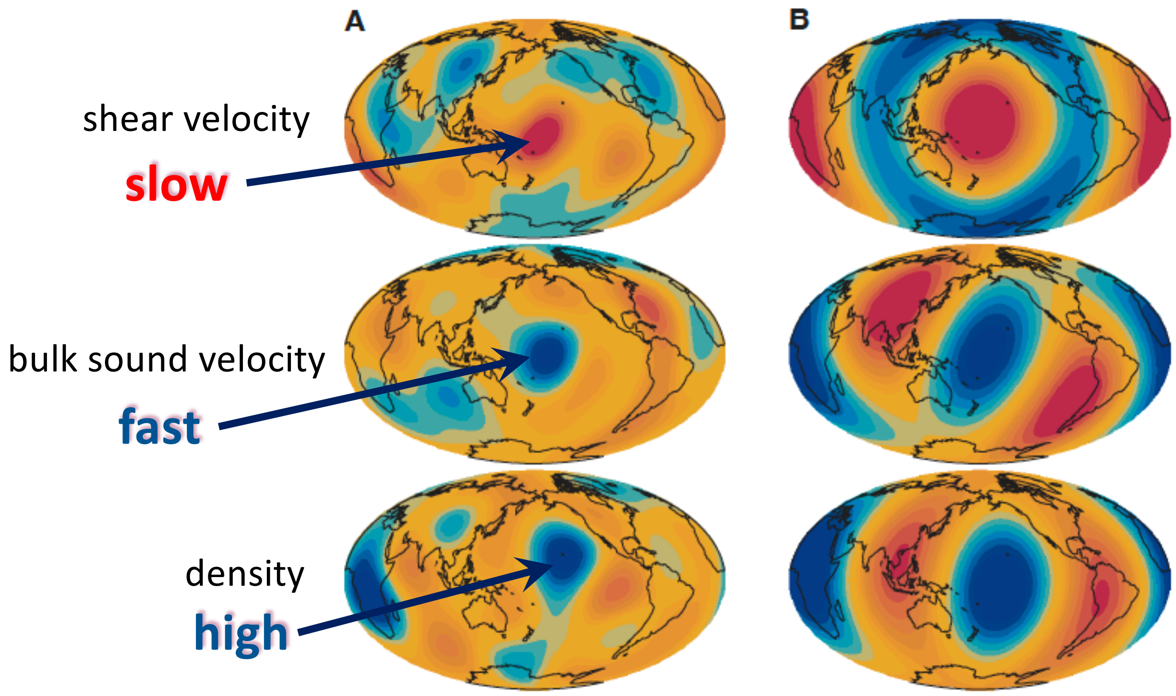

shear velocity

slow

bulk sound velocity

fast

density

high

spherical harmonic degrees 2,4,6

degree 2 only

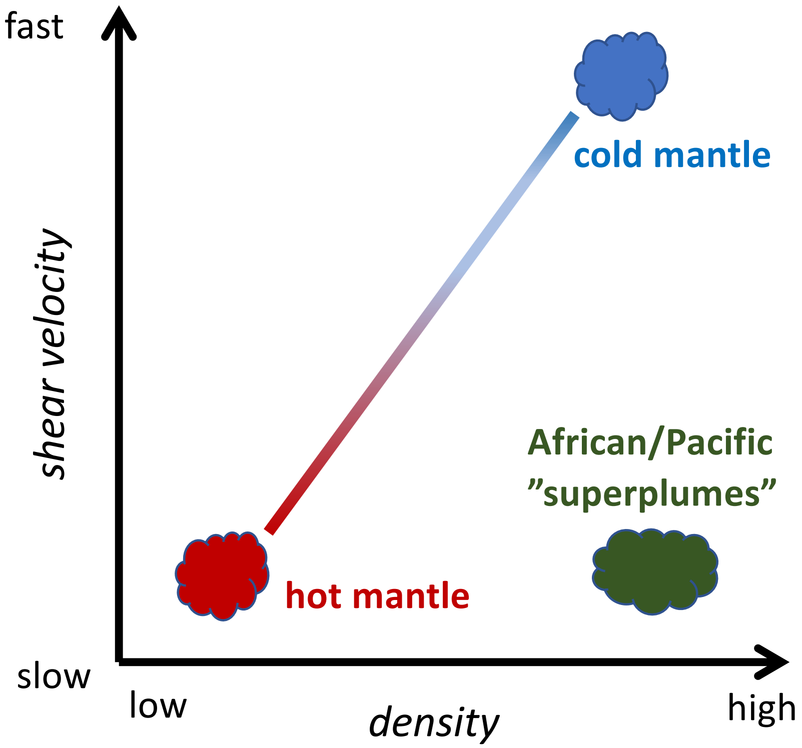

fast

slow

shear velocity

low

density

high

cold mantle

hot mantle

African/Pacific "superplumes"

→ **Large Low Shear Velocity Provinces**

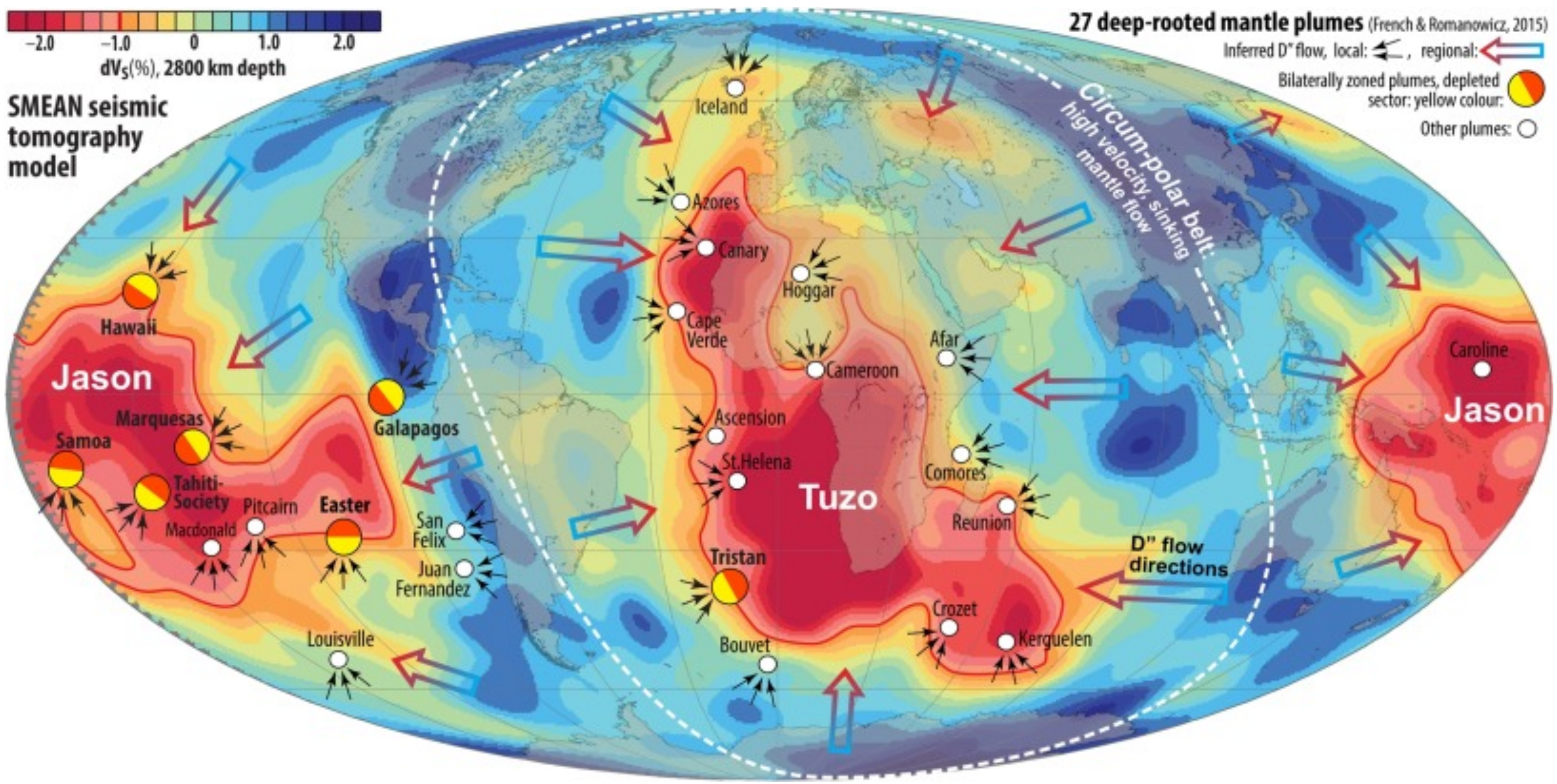
−2.0
−1.0
0
1.0
2.0
dV$_S$(%), 2800 km depth
SMEAN seismic tomography model
27 deep-rooted mantle plumes (French & Romanowicz, 2015)
Inferred D" flow, local: , regional:
Bilaterally zoned plumes, depleted sector: yellow colour:
Other plumes: ○
Circum-polar belt: high velocity, sinking mantle flow
Iceland
Azores
Canary
Hoggar
Cape Verde
Afar
Cameroon
Ascension
St.Helena
Comores
Reunion
Tuzo
Tristan
Crozet
Kerguelen
Bouvet
D" flow directions
Caroline
Jason
Hawaii
Jason
Marquesas
Samoa
Tahiti-Society
Macdonald
Pitcairn
Easter
Galapagos
San Felix
Juan Fernandez
Louisville

Detailed studies of seismic waveforms suggests LLSVPs may have sharp edges, supporting a chemical origin

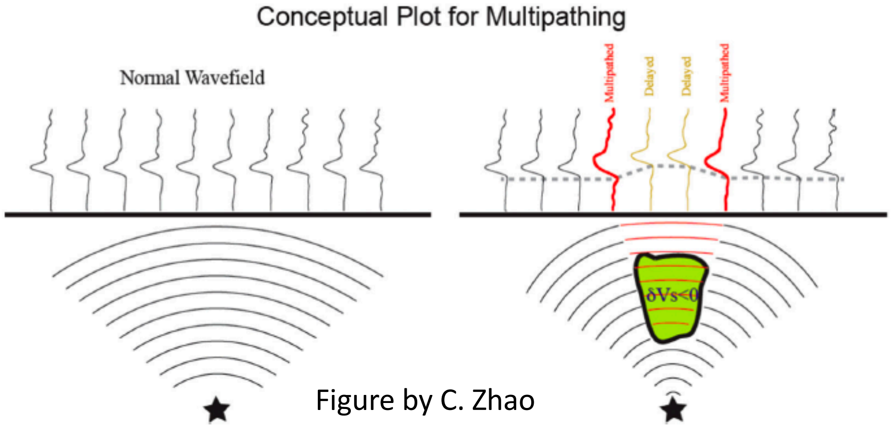

Figure by C. Zhao

McNamara, 2019

Hernlund & McNamara, 2015

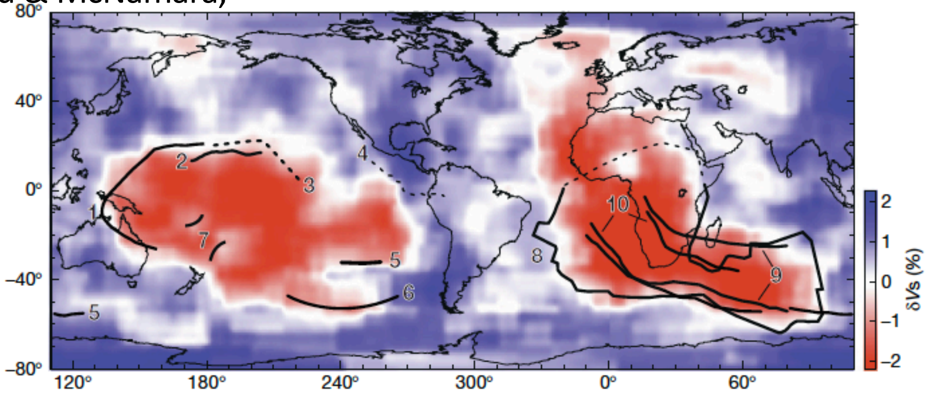

Figure 8 Map showing sharp edges of the large low-shear-wave-velocity provinces as inferred from travel-time and waveform seismic studies. The background map shows shear-wave tomography model TXBW (Grand, 2002). Sharp edges are represented as thick black lines, with dashed lines representing edges inferred from travel times. Numbers indicate the particular seismic studies (1. He et al. (2006); 2. Luo et al. (2001); 3. Breger and Romanowicz (1998); 4. Sun et al. (2007b); 5. To et al. (2005); 6. Ford et al. (2006a); 7. He and Wen (2009); 8. Wang and Wen (2004); 9. Sun et al. (2007b), Sun et al. (2009); and 10. Ni and Helmberger (2003c), Ni and Helmberger (2003a), and Ni and Helmberger (2003b)). This figure was provided by Ed Garnero and Chunpeng Zhao.

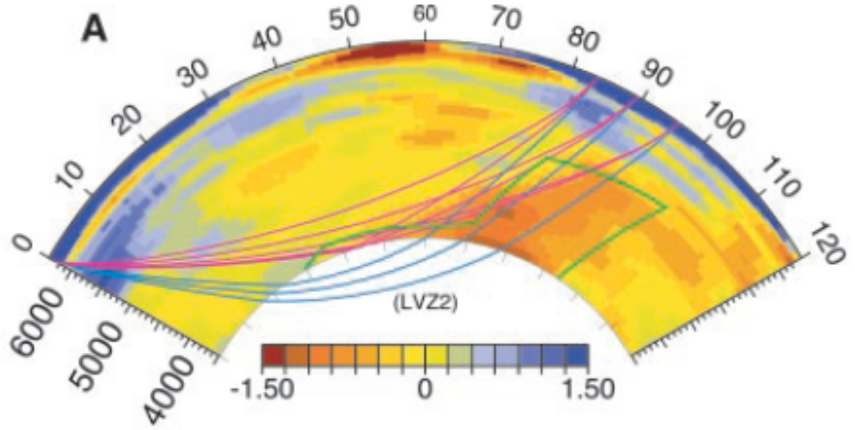

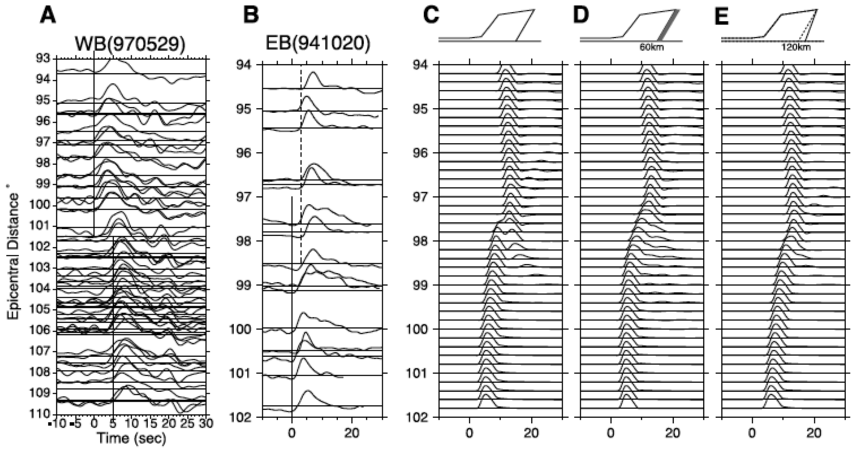

Ni et al., Science 2002

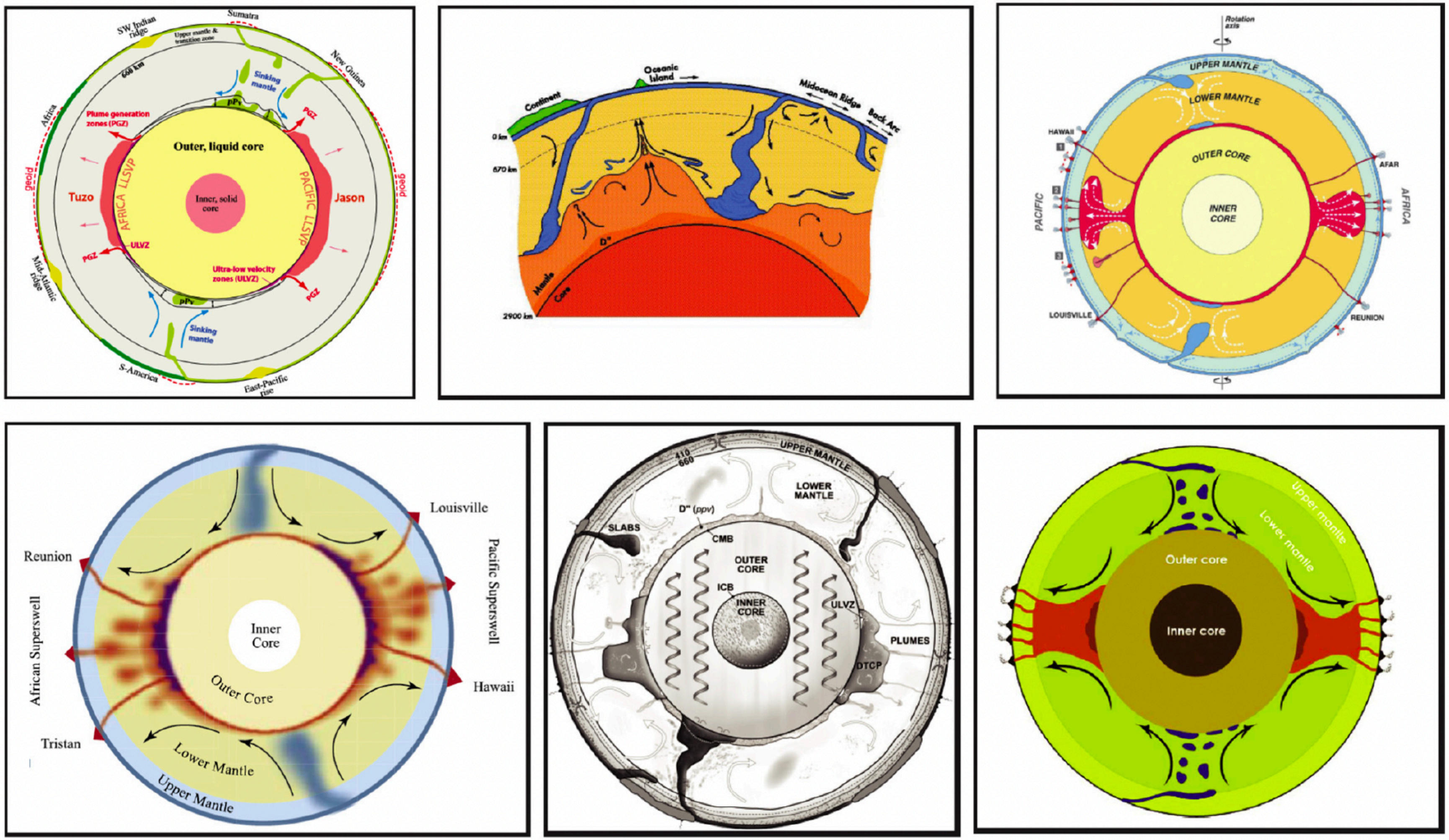

Fig. 1. Several conceptual models of mantle convection currently discussed in the solid-Earth community.
Figures are modified from the following sources, clockwise starting from the top left. **Top-left**: Torsvik et al. (2014). **Top-middle**: Kellogg et al. (1999). **Top-right**: Courtillot et al. (2003). **Bottom-left**: Jellinek and Manga (2004). **Bottom-middle**: Garnero et al. (2005). **Bottom-right**: Dziewonski et al. (2010).

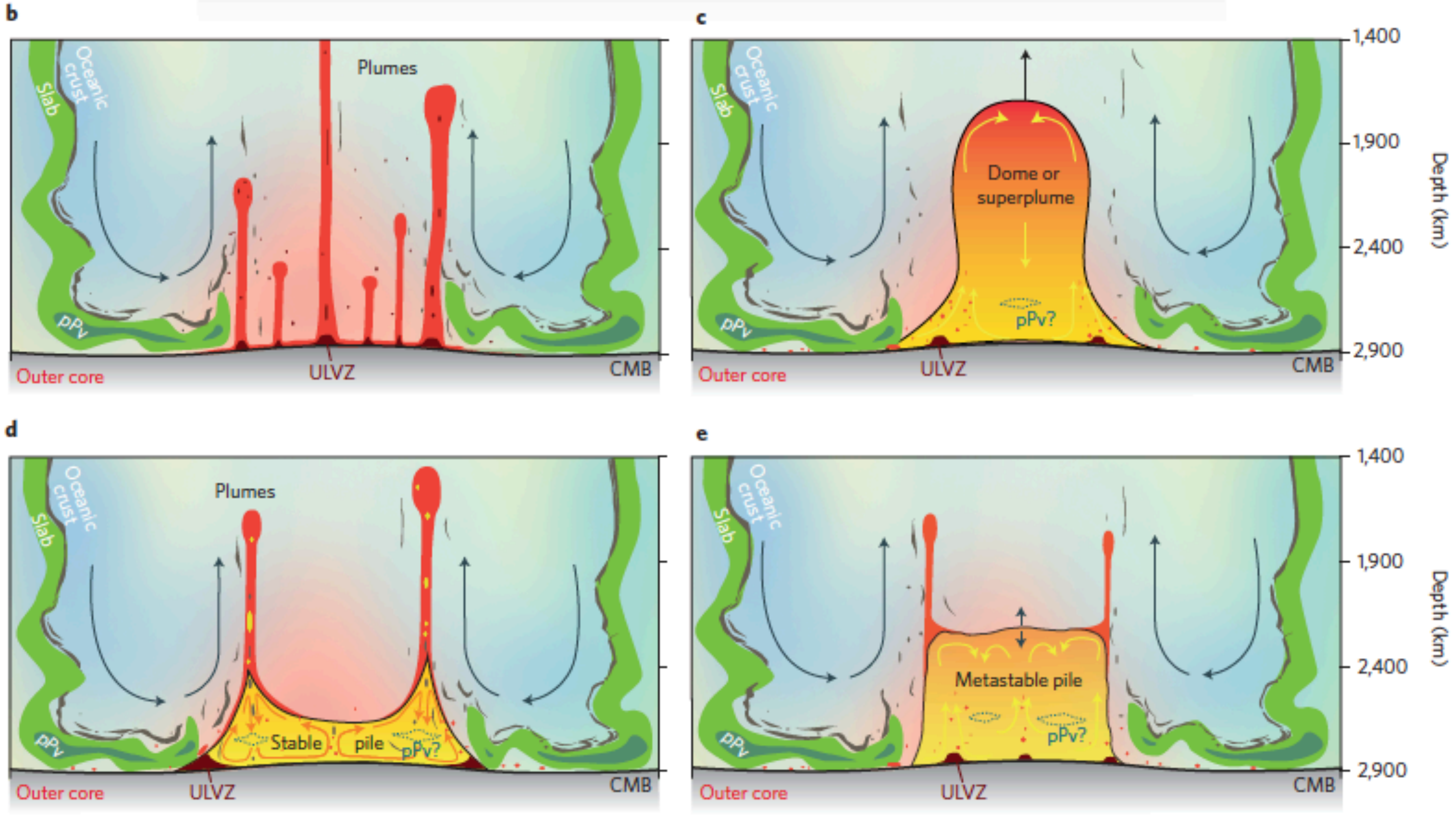

Figure 2 | LLSVP observations and interpretations. a, Surface features (upper panel) and seismically determined lower-mantle phenomena (lower panel). See text for details. **b–e**, Idealized possibilities proposed to explain LLSVPs. In all cases, subducted material (possibly including post-perovskite, pPv) surrounds the structure of interest that maps as the LLSVP. **b**, Plume cluster. **c**, Thermochemical superplume. **d**, Stable thermochemical pile. **e**, Metastable thermochemical pile. LIPs, large igneous provinces; CMB, core–mantle boundary; ULVZs, ultralow velocity zones.

Garnero et al., Nature Geoscience, 2016

Accumulations of subducted oceanic lithosphere?

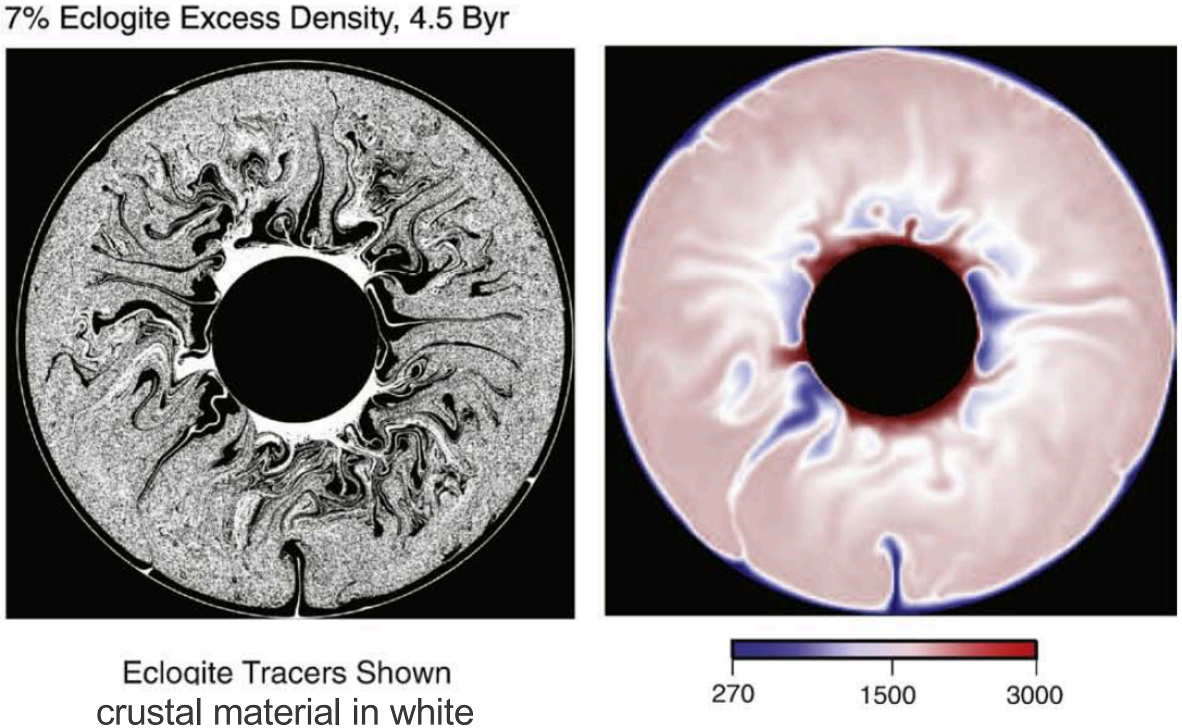

crustal material in white

Brandenburg et al., 2008

Primitive (primordial) material from Earth's early history?

(generally means enriched in Si and Fe)

McNamara, 2019

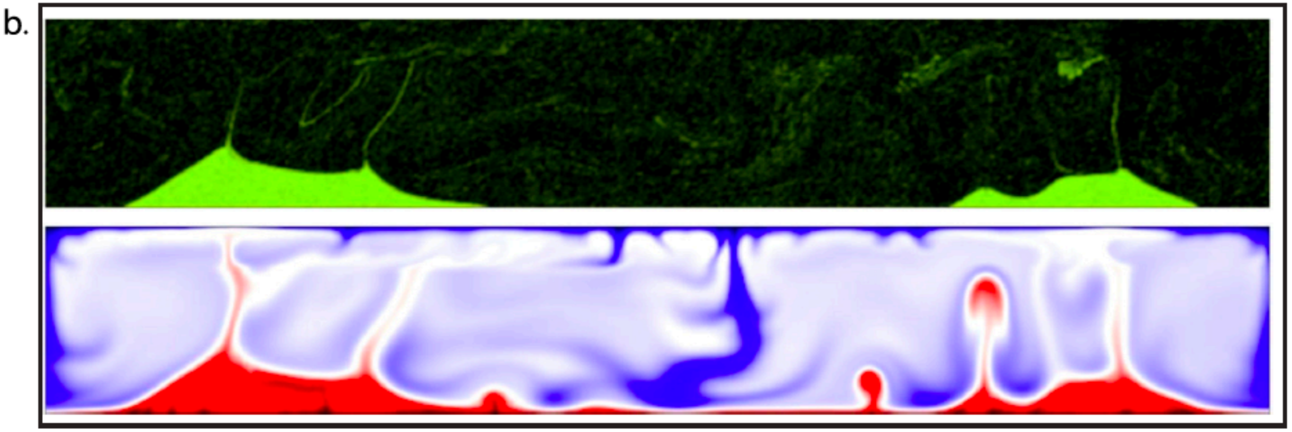

Compositional Field

Temperature Field

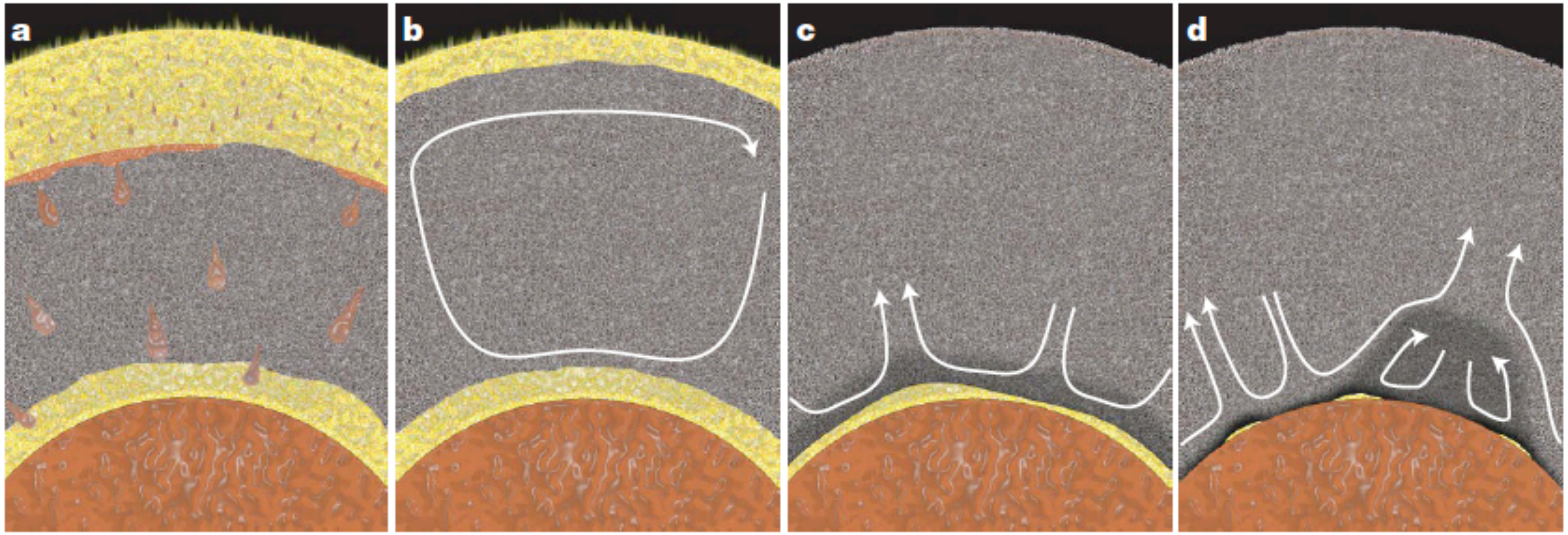

Basal magma ocean model

Labrosse et al., Nature 2007

Deschamps et al. EPSL 2012

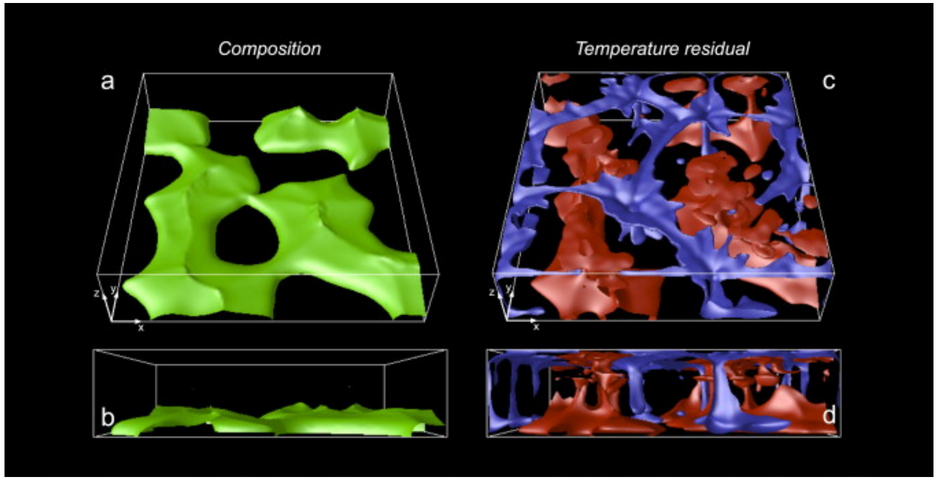

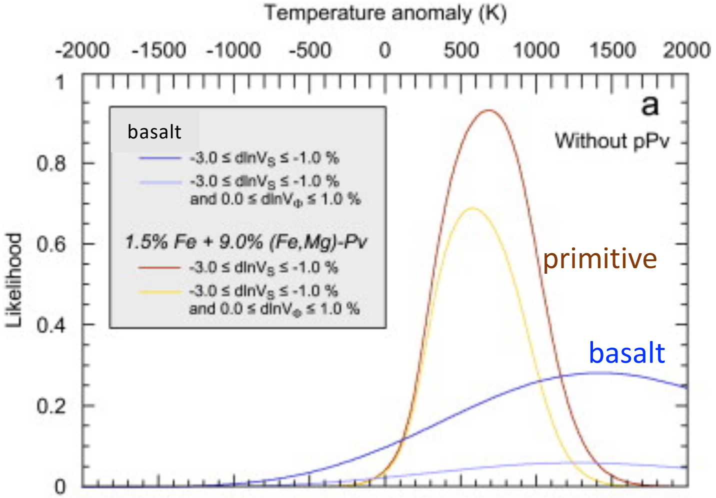

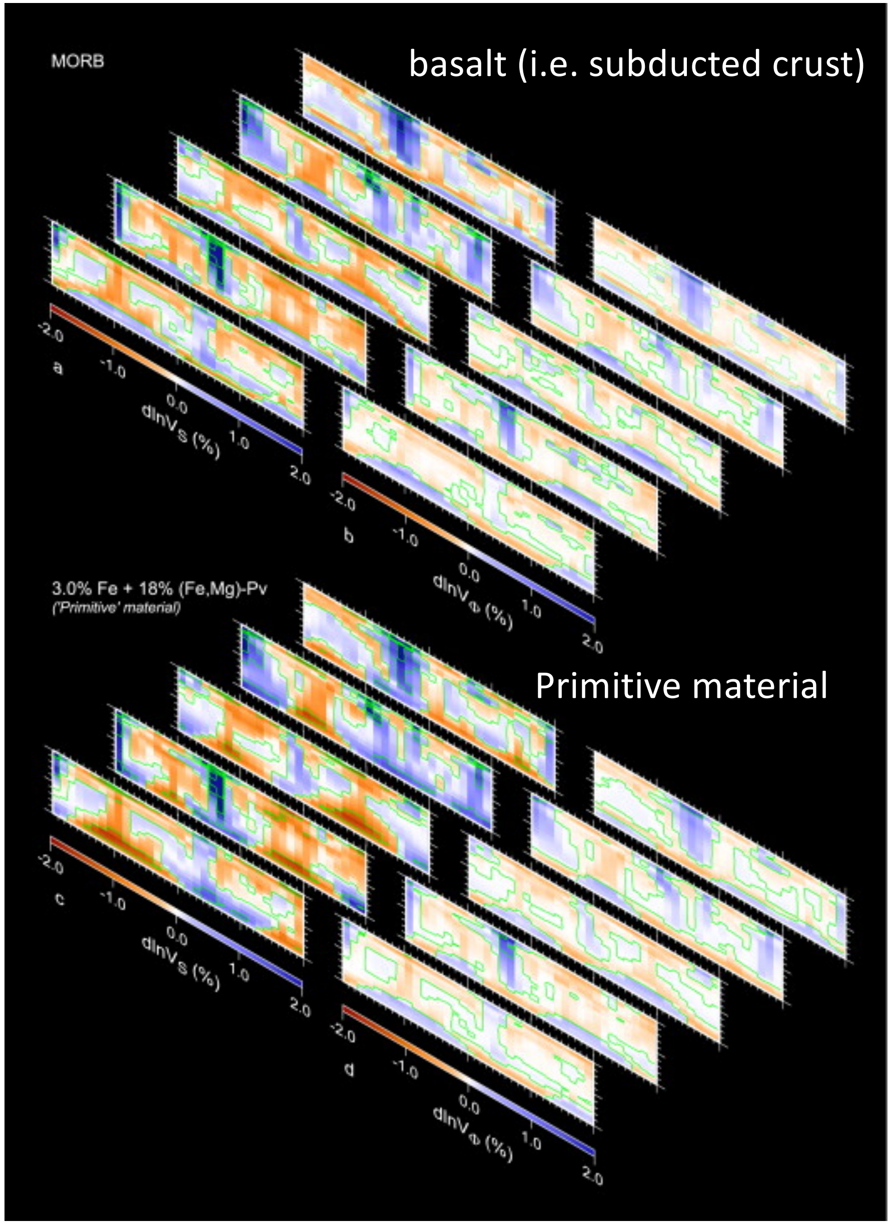

Redox reactions in a magma ocean

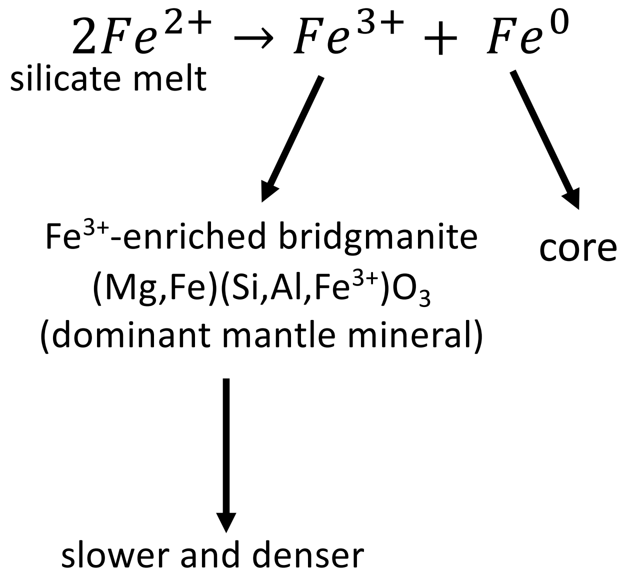

$2Fe^{2+} \rightarrow Fe^{3+} + Fe^{0}$

silicate melt

Fe^{3+}-enriched bridgmanite

$(Mg,Fe)(Si,Al,Fe^{3+})O_3$

(dominant mantle mineral)

core

slower and denser

Wang et al., Nature Communications 2021

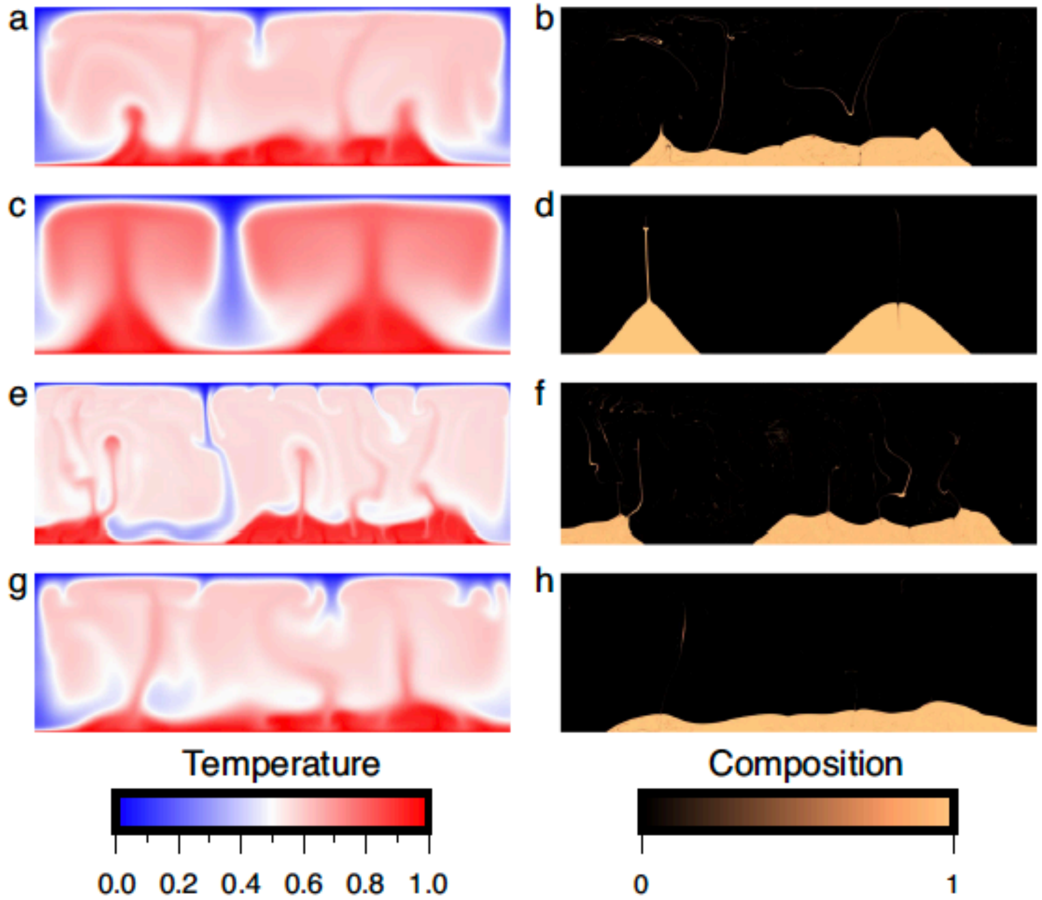

1.2% denser
Ra = $1x10^7$

1.2% denser
Ra = $1x10^6$

1.2% denser
Ra = $1x10^8$

1.5% denser
Ra = $1x10^7$

$$\underset{\text{bridgmanite}}{(Mg,Fe)(Si,Al)O_3} + \underset{\text{calcium perovskite}}{CaSiO_3} \xrightarrow{T > \sim 2300\ K} \underset{\text{Ca-rich bridgmanite}}{(Mg,Fe,Ca)(Si,Al)O_3}$$

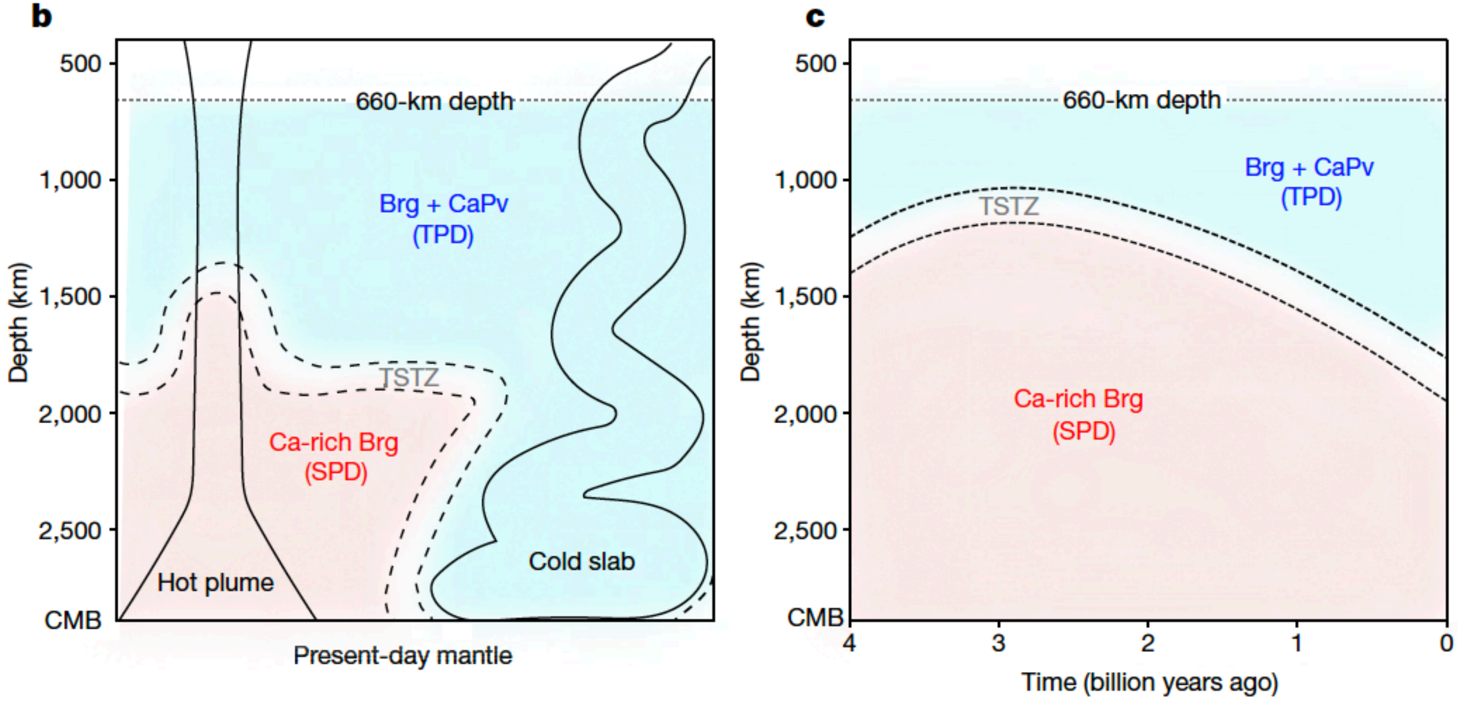

Ko et al., Nature 2022